the FEBS Journal

Loose interaction between glyceraldehyde-3-phosphate dehydrogenase and phosphoglycerate kinase revealed by fluorescence resonance energy transfer–fluorescence lifetime imaging microscopy in living cells

Yosuke Tomokuni[1], Kenji Goryo[1], Ayako Katsura[1], Satoru Torii[1], Ken-ichi Yasumoto[1], Klaus Kemnitz[2], Mamiko Takada[3], Hiroshi Fukumura[3] and Kazuhiro Sogawa[1]

1 Department of Biomolecular Sciences, Graduate School of Life Sciences, Tohoku University, Aoba-ku Sendai, Japan
2 EuroPhoton GmbH, Berlin, Germany
3 Department of Chemistry, Graduate School of Science, Tohoku University, Aoba-ku Sendai, Japan

Keywords
FLIM; FRET; GAPDH; loose interaction; PGK

Correspondence
K. Sogawa, Department of Biomolecular Sciences, Graduate School of Life Sciences, Tohoku University, Aoba-ku Sendai 980-8578, Japan
Fax: +81 22 795 6594
Tel: +81 22 795 6590
E-mail: sogawa@mail.tains.tohoku.ac.jp

(Received 14 April 2009, revised 7 December 2009, accepted 24 December 2009)

doi:10.1111/j.1742-4658.2010.07561.x

Loose interaction between the glycolytic enzymes glyceraldehyde-3-phosphate dehydrogenase (GAPDH) and phosphoglycerate kinase (PGK) was visualized in living CHO-K1 cells by fluorescence resonance energy transfer (FRET), using time-domain fluorescence lifetime imaging microscopy. FRET between active tetrameric subunits of GAPDH linked to cerulean or citrine was observed, and this FRET signal was significantly attenuated by coexpression of PGK. Also, direct interaction between GAPDH–citrine and PGK–cerulean was observed by FRET. The strength of FRET signals between them was dependent on linkers that connect GAPDH to citrine and PGK to cerulean. A coimmunoprecipitation assay using hemagglutinin-tagged GAPDH and FLAG-tagged PGK coexpressed in CHO-K1 cells supported the FRET observation. Taken together, these results demonstrate that a complex of GAPDH and PGK is formed in the cytoplasm of living cells.

Structured digital abstract

- MINT-7386555: *PGK* (uniprotkb:P00558) *physically interacts* (MI:0915) with *GAPDH* (uniprotkb:P04406) by *anti tag coimmunoprecipitation* (MI:0007)
- MINT-7386573: *GAPDH* (uniprotkb:P04406) and *PGK* (uniprotkb:P00558) *bind* (MI:0407) by *fluorescent resonance energy transfer* (MI:0055)
- MINT-7386590: *GAPDH* (uniprotkb:P04406) and *GAPDH* (uniprotkb:P04406) *bind* (MI:0407) by *fluorescent resonance energy transfer* (MI:0055)

Introduction

It has been demonstrated that consecutive enzymes in a number of metabolic pathways may form readily dissociable enzyme–enzyme complexes by which intermediary metabolites are directly transferred from one enzyme to the next without being released into the aqueous environment [1,2]. In the glycolytic and gluconeogenic pathways, pairs of enzymes – aldolase and glyceraldehyde-3-phosphate dehydrogenase (GAPDH), GAPDH and phosphoglycerate kinase (PGK), GAPDH and lactate dehydrogenase, and aldolase and fructose-1,6-bisphosphatase – are reported to form loose complexes [1,2]. Of these enzyme pairs, GAPDH and PGK constitute the sixth and seventh reactions in the glycolytic pathway. GAPDH is a homotetramer with a

Abbreviations
DAPI, 4′,6-diamidino-2-phenylindole; FLIM, fluorescence lifetime imaging microscopy; FRET, fluorescence resonance energy transfer; GAPDH, glyceraldehyde-3-phosphate dehydrogenase; GFP, green fluorescent protein; HA, hemagglutinin; IRF, instrumental response function; PGK, phosphoglycerate kinase; TRITC, tetramethylrhodamine isothiocyanate.

subunit size of 34 000–38 000 Da, and PGK acts as a monomer with a molecular mass of 44 000 Da. In most bacteria, the genes encoding these two enzymes form an operon, and in animals, the two enzymes, together with some other glycolytic enzymes, are upregulated by hypoxic stress [3,4].

The dynamic complex has been hard to demonstrate, as enzyme–enzyme complexes are not stable and are thus not isolatable. Several lines of evidence for the presence of the GAPDH–PGK complex were obtained by *in vitro* biochemical studies using concentrated, purified enzymes. Association of PGK with GAPDH was demonstrated by utilizing gel penetration analysis or by using immobilized GAPDH on CNBr-activated Sepharose [5–7]. Interaction between the enzymes was observed by measuring changes in the fluorescence intensity of fluorescein isothiocyanate-labeled PGK in the presence or absence of GAPDH [8]. Furthermore, Weber and Bernhard presented kinetic evidence obtained using purified enzymes from rabbit muscle for substrate channeling through the complex of GAPDH and PGK [9]. However, it was also reported that the complex was easily decomposed by changes in experimental conditions, such as pH shifts or increased salt concentrations. Several conflicting results were also reported that argued against the existence of the complex and channeling of metabolites [10,11]. Thus, the existence of the complex has not been universally accepted. In addition to the cytoplasmic compartment, GAPDH and PGK are known to form a functional complex at synaptic vesicles in neurons and sarcoplasmic membranes in muscle cells for local ATP production that is tightly coupled with their membrane transport function [12,13].

Determination of fluorescence resonance energy transfer (FRET) between two fluorescent proteins using fluorescence lifetime imaging microscopy (FLIM) is a technique for the observation of protein–protein interactions [14,15]. This method can be applied to interactions in loose complexes in living cells, and has an advantage in that the FRET strength is solely dependent upon the distance between and relative orientation of two fluorophores, being independent of the strength of protein–protein interactions. In the case of very weak interactions as described in this article, rapid association and dissociation of FRET pairs may also reduce FRET efficiency. We applied this FRET–FLIM technique to direct observation of the interaction between GAPDH and PGK chimeric proteins linked to cerulean [16] or citrine [17], a FRET pair, in living cells.

Results and Discussion

Effect of PGK on the interaction between subunits of GAPDH

Expression plasmids for GAPDH and PGK linked to cerulean or citrine were introduced into CHO-K1 cells. As shown in Figs 1A and S1A, transiently expressed GAPDH–citrine (chimeric protein with N-terminal GAPDH and C-terminal citrine) and citrine–GAPDH (chimeric protein with N-terminal citrine and C-terminal GAPDH) were localized in the cytoplasm. PGK–cerulean (chimeric protein with N-terminal PGK and C-terminal cerulean) and cerulean–PGK (chimeric protein with N-terminal cerulean and C-terminal PGK) were present throughout the cell. These results agree with the subcellular localization of endogeneous GAPDH and PGK in HeLa cells (Fig. 1A). These proteins were resolved by size exclusion column chromatography (Figs 1B,C and S1B,C). GAPDH–citrine and citrine–GAPDH were eluted at the position corresponding to tetramers, and no tetramers containing chimeric proteins and endogenous GAPDH monomers were found, suggesting that the interfaces needed for the formation of tetramers are mutually incompatible between human and Chinese hamster GAPDH (Figs 1B and S1B). A similar result was obtained when cell extracts containing GAPDH–cerulean (chimeric protein with N-terminal GAPDH and C-terminal cerulean) or cerulean–GAPDH (chimeric protein with N-terminal cerulean and C-terminal GAPDH) were analyzed by chromatography (Fig. S1). Chimeric proteins of PGK and cerulean were eluted at the position corresponding to monomers (Figs 1C and S1C). It is not clear why endogenous PGK activity showed a broad peak.

The decay curve of cerulean–GAPDH was analyzed by two-exponential fitting (Fig. 2). Lifetimes of cerulean–GAPDH were calculated to be 1.41 and 3.59 ns, with fraction ratios of 36.8% and 63.2%, respectively (Table 1). This fluorescence decay was considerably accelerated in the presence of citrine–GAPDH by energy transfer (Fig. 2B). Short and long lifetimes, τ_1 and τ_2, were reduced to 1.06 and 3.13 ns, respectively. In order to examine the stability of the instrument, the fluorescence of cerulean–GAPDH was repeatedly measured. As shown in Fig. 2C, the second decay curve completely overlapped with the first one. We also repeatedly measured the donor fluorescence of cells expressing cerulean–GAPDH and citrine–GAPDH after sequential measurements of donor and acceptor fluorescence (Fig. 2C). Perfectly overlapped decay curves for the first and second measurements

were obtained. These results indicate that the FLIM apparatus used in this study had enough stability for the FLIM measurements, and suggest that minimal photodynamic reactions such as photobleaching occurred in the live cells during measurements. Fluorescence corresponding to a reduction in donor lifetimes was observed in the decay curve of acceptors (Fig. 2B). The FRET signal was decreased by the coexpression of PGK (Fig. 2D), and corresponding to this reduction, a fluorescence rise in the decay curve of citrine–GAPDH was hardly observed (Fig. 2D). This attenuated FRET signal suggests that the binding of PGK resulted in a conformational change of GAPDH tetramers to separate donors and acceptors. Representative fluorescence lifetime images, which were produced by single-exponential fitting, were shown in Fig. 2E. Lifetimes of cerulean–GAPDH were similar all over the cell except for the nucleus, in which cerulean–GAPDH was not expressed and no lifetimes were exhibited. The lifetimes in the cytoplasm were reduced by the coexpression of citrine–GAPDH, but coexpression of PGK did not affect the lifetimes. Coexpression of citrine–GAPDH and PGK weakly decreased the lifetimes of cerulean–GAPDH in the cytoplasm, confirming the results shown in Fig. 2B,D. The lifetimes analyzed by the two-exponential fitting are summarized in Table 1. During FRET measurements, very weak background signals (below 5% of donor fluorescence intensity) due to autofluorescence of CHO-K1 cells were observed (data not shown). Chi-square values of the fitting were between 1.0 and 1.2, as shown in Table 1. Using a typical decay result, the chi-square value was plotted against the lifetime as shown in

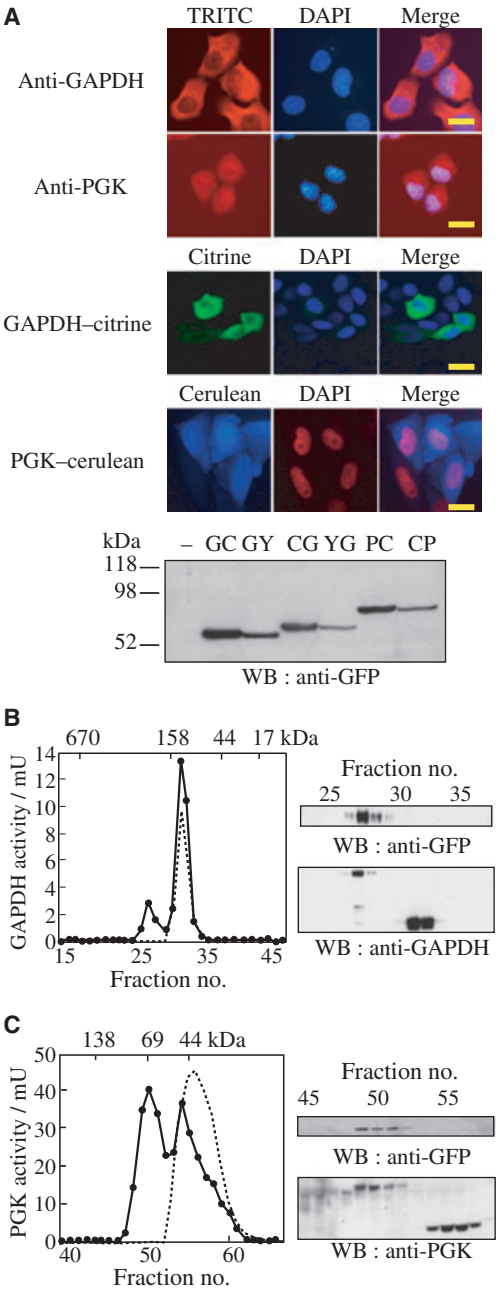

Fig. 1. Subcellular localization and enzymatic activities of GAPDH–citrine and PGK–cerulean. (A) Expression of GAPDH–citrine and PGK–cerulean. Localization of endogenous GAPDH and PGK in HeLa cells was examined by using antibodies against GAPDH and PGK, respectively, followed by incubation in TRITC-conjugated secondary antibody. Chimeric proteins, GAPDH–citrine and PGK–cerulean, were transiently expressed in CHO-K1 cells by DNA transfection, using the lipofection method. Forty hours after transfection, fluorescence of cerulean and citrine moieties of the chimeric proteins was observed with an Olympus BX50 fluorescent microscope with a filter set (Olympus U-MCFPHQ and U-MYFPHQ). Scale bars: 20 μm. The fluorescent color of 4′,6-diamidino-2-phenylindole (DAPI) in the cells expressing PGK–cerulean was changed from blue to red on a computer. The results of western blot (WB) analysis using whole cell extracts of cells transfected with plasmids for GAPDH–cerulean (GC), GAPDH–citrine (GY), cerulean–GAPDH (CG), citrine–GAPDH (YG), PGK–cerulean (PC) and cerulean–PGK (CP) are shown. (B, C) Size exclusion chromatography of whole cell extracts with expression of GAPDH–citrine (B) and PGK–cerulean (C). Cell extracts (0.15 mL) of CHO-K1 cells were applied to a column (Waters Superdex 200 for GAPDH and Superdex 75 for PGK; 1 × 30 cm). Elution was performed at room temperature at a flow rate of 0.4 mL·min^{-1} with Hepes/NaOH buffer (pH 7.9). Fractions of 0.4 mL were collected. Thyroglobulin (670 kDa), γ-globulin (158 kDa), serum albumin dimer (138 kDa), serum albumin (69 kDa), ovalbumin (44 kDa) and myoglobin (17 kDa) were used as size markers. Determination of enzyme activity for GAPDH and PGK and immunoblot analysis were performed as described in Experimental procedures. Filled circles show the activity of cells transfected with plasmids for chimeric proteins. Endogenous GAPDH and PGK activity from untransfected cells are shown as dashed lines.

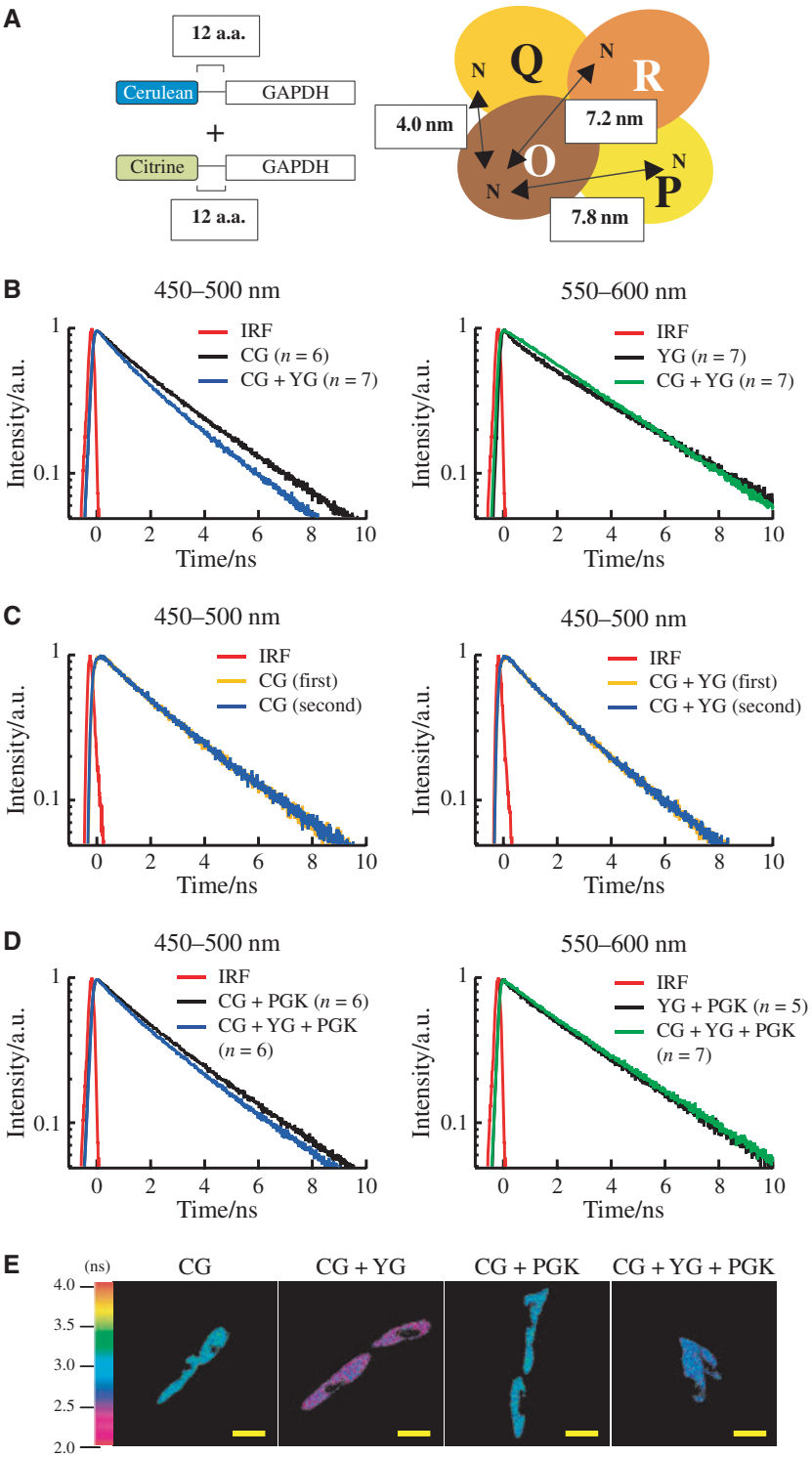

Fig. 2. FRET between cerulean–GAPDH and citrine–GAPDH monomers constituting hybrid tetramers. (A) Structure of fluorescent chimeric GAPDH proteins and tetrameric structure of GAPDH. The structure of chimeric proteins is schematically shown on the left. The linker peptide connecting cerulean or citrine to GAPDH is 12 amino acids long, with the sequence SGLRSRAQASNS. The tetrameric structure of GAPDH is schematically shown on the right. The distances between the N-terminal amino acids of subunits O and P, subunits O and Q and subunits O and R are shown (B–D). FLIM analysis of the interaction between cerulean–GAPDH and citrine–GAPDH in living CHO-K1 cells. CHO-K1 cells were transfected with plasmids encoding cerulean–GAPDH (CG) and citrine–GAPDH (YG), together with a plasmid for PGK (D) or with pCMV vector with no insert (B). The fluorescence decay curves of cerulean (blue) and citrine (green) represent an average of fluorescence decay data obtained from the cytoplasmic area of the observed cells. The decay curve of separately expressed cerulean–GAPDH and citrine–GAPDH (black) in the presence or absence of coexpressed PGK is also shown. The shapes of the recorded IRF are shown in red. Experiments were performed at least three times, and representative results from one experiment are shown. A typical result of repeated measurements of cerulean–GAPDH fluorescence is also shown in (C). After sequential measurement of cerulean–GAPDH and citrine–GAPDH, a second measurement was performed on the same cell, and decay curves obtained from the first (shown in red) and second measurements (shown in blue) are shown. (E) FLIM images of cerulean–GAPDH in the presence of citrine–GAPDH and/or PGK. A lifetime map was made from time-correlated single-photon-counting data by fitting the data to a single exponential decay. In the FLIM map, color corresponds to the fluorescence lifetime indicated by a false color scale. Scale bars: 20 μm.

Fig. S2. The chi-square values used for Table 2 showed minimal values of the curves, suggesting that the two-exponential fitting of the decay curves was performed properly.

Interaction between GAPDH and PGK

Changes in the FRET signals observed above suggest a direct interaction between GAPDH and PGK. Direct

Table 1. Fluorescence decay data for cerulean–GAPDH in the presence or absence of citrine–GAPDH and/or PGK expressed in living CHO-K1 cells. a_1 and a_2 are the exponential coefficients for the τ_1 and τ_2 decay times, respectively. *n*, number of cells examined.

Protein combination	a_1 (%)	τ_1 (ns)	a_2 (%)	τ_2 (ns)	*n*	χ^2
Cerulen–GAPDH	36.8	1.41 ± 0.21[a]	63.2	3.59 ± 0.13[a]	6	1.0–1.1
Cerulean–GAPDH Citrine–GAPDH	39.6	1.06 ± 0.09[a,b]	60.4	3.13 ± 0.07[a,b]	6	1.0–1.1
Cerulean–GAPDH PGK	39.9	1.43 ± 0.20	60.1	3.63 ± 0.19	6	1.0–1.2
Cerulean–GAPDH Citrine–GAPDH PGK	41.4	1.29 ± 0.05[b]	58.6	3.44 ± 0.10[b]	6	1.0–1.1

[a] The differences between the two τ_1 values and the two τ_2 values were significant ($P < 0.005$ for τ_1 and $P < 0.001$ for τ_2). [b] The differences between the two τ_1 values and the two τ_2 values were significant ($P < 0.001$).

Table 2. Fluorescence decay data for PGK–cerulean in the presence or absence of GAPDH–citrine expressed in living CHO-K1 cells. a_1 and a_2 are the exponential coefficients for the τ_1 and τ_2 decay times, respectively. Data are derived from the whole area (in the case of cell samples without coexpression of GAPDH) or from the cytoplasmic area (in the case of cell samples with coexpression of GAPDH) of cells, and are expressed as mean ± standard deviation. *n*, number of cells examined.

Protein combination	a_1 (%)	τ_1 (ns)	a_2 (%)	τ_2 (ns)	*n*	χ^2
PGK–5aa–cerulean	37.1	1.39 ± 0.05[a]	62.9	3.62 ± 0.05[a]	6	1.0–1.2
PGK–5aa–cerulean GAPDH–5aa–citrine	42.2	1.19 ± 0.07[a]	58.8	3.27 ± 0.14[a]	6	0.8–1.0
PGK–7aa–cerulean	43.4	1.32 ± 0.05[c]	56.6	3.46 ± 0.09[c]	6	1.0–1.1
PGK–7aa–cerulean GAPDH–7aa–citrine	43.8	1.33 ± 0.05[c]	56.2	3.39 ± 0.11[c]	5	1.0–1.1
PGK–10aa–cerulean	31.2	1.37 ± 0.06[b]	68.8	3.56 ± 0.06[b]	6	0.9–1.1
PGK–10aa–cerulean GAPDH–10aa–citrine	41.1	1.24 ± 0.12[b]	58.9	3.31 ± 0.11[b]	7	0.9–1.0

[a] The differences between the two τ_1 values and the two τ_2 values were significant ($P < 0.001$). [b] The differences between the two τ_1 values and the two τ_2 values were significant ($P < 0.05$ for τ_1 and $P < 0.001$ for τ_2). [c] The differences between the two τ_1 values and the two τ_2 values were not significant ($P > 0.05$).

interaction between the two enzymes was determined by the simultaneous expression of GAPDH–citrine and PGK–cerulean. We expressed three pairs of chimeric proteins to determine FRET signals with different sizes of linkers connecting GAPDH or PGK to fluorescent proteins (Fig. 3). These proteins were relatively evenly expressed, as shown in Fig. 3D. FRET signals were observed between GAPDH–citrine and PGK–cerulean only when fluorescent proteins and enzymes were connected with linkers of five or 10 amino acids, and not when they were linked by seven amino acids. In agreement with this result, lifetimes of PGK–5aa–cerulean and PGK–10aa–cerulean expressed in the cytoplasm, but not in the nucleus, were reduced when acceptors, GAPDH–5aa–citrine and GAPDH–10aa–citrine, respectively, were coexpressed as shown in the FLIM images (Fig. 3A,C) and in Table 2. On the other hand, the lifetimes of PGK–7aa–cerulean and their intracellular distribution remained unchanged when GAPDH–7aa–citrine was coexpressed (Fig. 3B and Table 2). This finding indicates that induction of FRET does not simply depend on the length of linkers. In the linker containing seven amino acids, a Pro-Pro sequence that is not contained in other linkers is incorporated. This less flexible structure may inhibit fluorophores to allow an orientation and a position suitable for energy transfer. In agreement with these data, coimmunoprecipitation experiments in whole CHO-K1 cell extracts demonstrated a specific interaction of GAPDH with PGK, albeit at very low efficiency (Fig. 3E). Although we also examined FRET signals using the other combinations of GAPDH and PGK, GAPDH–citrine versus cerulean–PGK, citrine–GAPDH versus cerulean–PGK, and citrine–GAPDH versus PGK–cerulean, no FRET signals were obtained (data not shown).

Lifetimes of fluorescent proteins in living cells can be changed without energy transfer to acceptor fluorescent proteins. Tramier *et al.* reported that lifetimes of cyan fluorescent protein in living cells can be changed under strong illumination by a mercury lamp [18]. It is also possible for energy transfer to occur from donors to endogenous acceptors such as flavins. In addition to lifetime measurements of donors, analysis of the decay curve of the acceptor may eliminate possible errors. We analyzed fluorescent decay curves of the acceptor and obtained, in almost all cases, a clear fluorescence rise in the curve corresponding to the extent of reduction of donor lifetimes. A detailed analysis of fluorescence rise in the acceptor decay curve revealed that it is included as a negative component with the same lifetime as that of the FRET component in the donor curve (M. Takada *et al.*, unpublished observation).

Besides glycolysis and gluconeogenesis, GAPDH and PGK have different functions in the nucleus. PGK acts

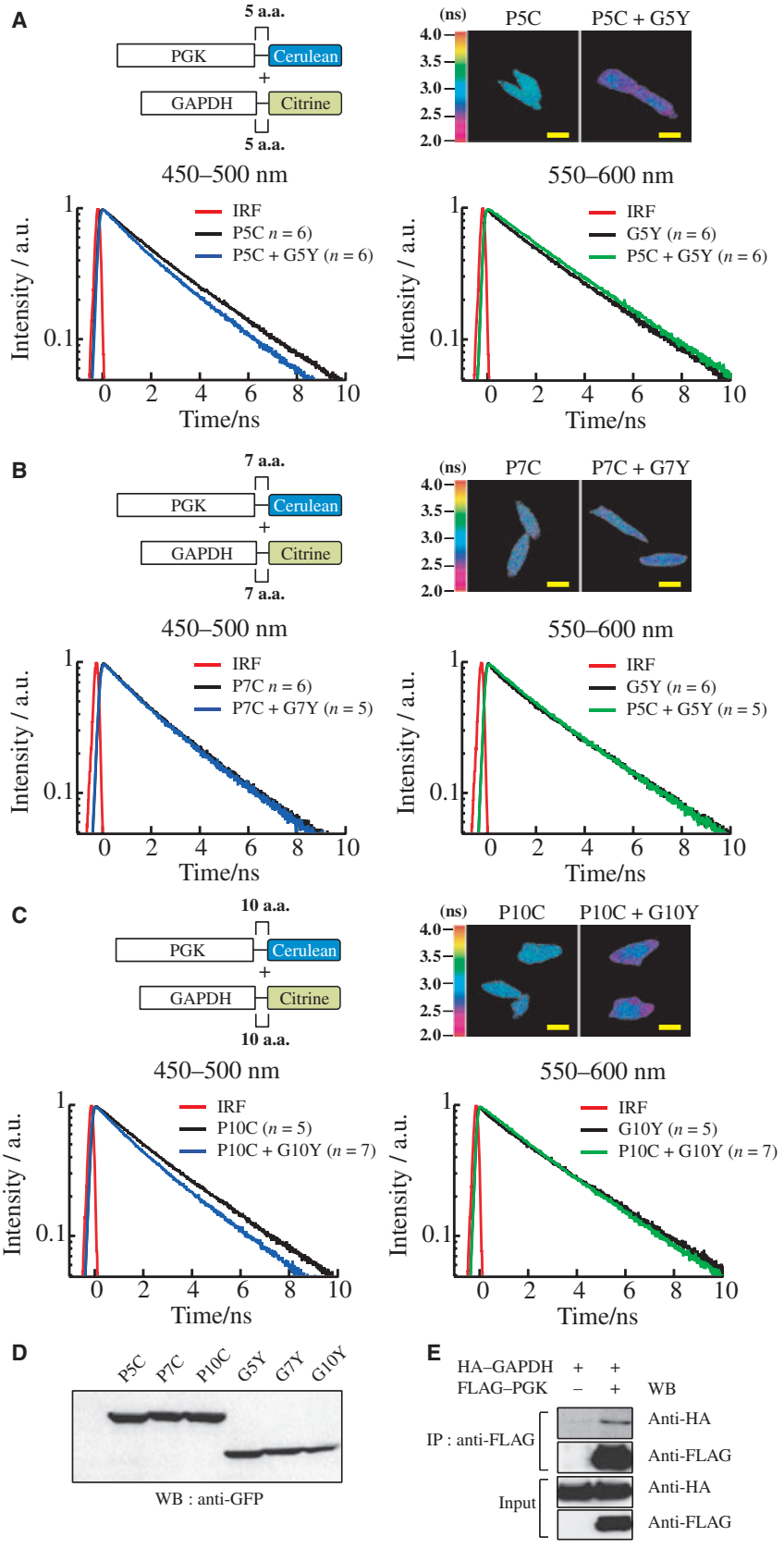

Fig. 3. Interaction between PGK–cerulean and GAPDH–citrine. Chimeric plasmids for PGK linked to cerulean and GAPDH linked to citrine with different lengths of linker peptides were constructed and introduced into CHO-K1 cells: (A) five amino acids (TPVAT for GAPDH; MPVAT for PGK); (B) seven amino acids (TDPPVAT for GAPDH; MDPPVAT for PGK); and (C) 10 amino acids (TDPGAGPVAT for GAPDH; MDPGAGPVAT for PGK). P5C, PGK–5aa–cerulean; G5Y, GAPDH–5aa–citrine; P7C, PGK–7aa–cerulean; G7Y, GAPDH–7aa–citrine; P10C, PGK–10aa–cerulean; G10Y, GAPDH–10aa–citrine. The fluorescence decay curves of cerulean (blue) and citrine (green) represent an average of fluorescence decay data obtained from the cytoplasmic area of the observed cells. For comparison, the decay curve of PGK–cerulean without acceptor (left, black) and GAPDH–citrine without donor (right, black) is also shown. The shapes of the recorded IRF are shown in red. Experiments were separately performed at least three times, and representative results from one experiment are shown. FLIM images of donors and donors coexpressed with acceptors are shown on the right. Lifetime maps were made from time-correlated single-photon-counting data by fitting data to a single exponential decay. In the FLIM maps, color corresponds to the fluorescence lifetime indicated by a false color scale. Scale bars: 20 μm. (D) Expression of PGK and GAPDH chimeric proteins. Expression plasmids were transfected into CHO-K1 cells, and proteins were subjected to SDS/PAGE, transferred to nitrocellulose membranes, and probed with antibody against GFP. (E) Coimmunoprecipitation analysis of GAPDH and PGK in cell extracts obtained from CHO-K1 cells transfected with expression plasmids for HA–GAPDH and FLAG–PGK; 0.7% input is shown.

as a primer recognition protein, a cofactor of DNA polymerase α [19]. GAPDH has a uracil DNA glycosylase activity [20] and has substantial involvement in apoptosis in neural cells through interaction with p53 [21]. A tight association between GAPDH and PGK would inhibit these functions, although convincing evidence for the existence of independent entities in such functions was not presented. Loose interaction between the two enzymes enables interactions of an enzyme with other proteins that are necessary for these functions.

The dynamic complex is difficult to demonstrate, because of its inherent instability. Our FRET–FLIM system may serve as a valuable tool for investigating weak interactions in the complex in living cells.

Experimental procedures

Plasmid construction

Human full-length GAPDH cDNA was cloned from a cDNA library of HepG2 cells. Human PGK cDNA (pQE16–hPGK1) was kindly provided by K. Mizumoto (Kitasato University), and pcerulean-N1, pcerulean-C1, pcitrine-N1 and pcitrine-C1 were constructed by site-directed mutagenesis, using corresponding plasmids for cyan fluorescent protein and yellow fluorescent protein as templates. For the construction of pcerulean–hGAPDH or pcitrine–hGAPDH, cDNA for GAPDH was amplified by PCR, using the synthetic oligonucleotides 5′-CGGAA TTCCA TGGGG AAGGT GAAGG TCGG-3′ and 5′-GGCGG ATCCT TACTC CTTGG AGGCC ATGTG GG-3′ as primers. After digestion of the synthesized fragment by *Eco*RI and *Bam*HI, the fragment was inserted between the *Eco*RI and *Bam*HI sites of pcerulean-C1 or pcitrine-C1. phGAPDH–7aa–citrine and phGAPDH–5aa–citrine were similarly constructed using the primers 5′-CGG AA TTCCG ATGGG GAAGG TGAAG GTCGG-3′ and 5′-CGGAA TTCCG ATGGG GAAGG TGAAG GTCG G-3′, and 5′-CGGAA TTCCG ATGGG GAAGG TGA AG GTCGG-3′ and 5′-CGACC GGTGT CTCCT TGG AG GCCAT GTGGG-3′, respectively, and pcitrine-N1. phPGK1–7aa–cerulean and phPGK1–5aa–cerulean were constructed using the primers 5′-CCGGA ATTCC AATGT CGCTT TCTAA CAAGC T-3′ and 5′-GGCGG ATCCA TAATA TTGCT GAGAG CATCC A-3′, and 5′-CCGGA ATTCC AATGT CGCTT TCTAA CAAGC T-3′ and 5′-CGACC GGTAT AATAT TGCTG AGAGC ATCCA-3′, respectively, and pQE16–hPGK1 as template DNA. After digestion of the synthesized fragment by *Eco*RI and *Bam*HI, the resulting fragments were inserted between the *Eco*RI and *Bam*HI sites of pcerulean-N1. pcerulean–hPGK1 was constructed using the primers 5′-CCGGA ATTCG ATGTC GCTTT CTAAC AAGCT-3′ and 5′-GGCGG ATCCT TAAAT ATTGC TGAGA GCATC C-3′, and pcerulean-C1. For the construction of phGAPDH–10aa–citrine, the synthetic oligonucleotides 5′-GATCC GGGCG CCGGA-3′ and 5′-CCGGT CCGGC GCCCG-3′ were inserted between the *Age*I and *Bam*HI sites of phGAPDH–7aa–citrine. phPGK1–10aa–cerulean was similarly constructed using the synthetic oligonucleotides 5′-GATCC GGGCG CCGGA-3′ and 5′-CCGGT CCGGC GCCCG-3′, and phPGK1–7aa–cerulean. pCMV–hGAPDH was constructed by self-ligation of the blunt-ended *Age*I–*Bsp*EI fragment of pcerulean–hGAPDH. pCMV–hPGK1 was similarly constructed using pcitrine–hPGK1. pBOS–hemagglutinin (HA)–hGAPDH and pBOS–FLAG–hPGK1 were constructed by inserting the blunt-ended *Eco*RI–*Bam*HI fragments of pcerulean–hGAPDH and pcerulean–hPGK1 into the *Eco*RV site of pBOS–HA and pBOS–FLAG vectors, respectively. All plasmid constructs were verified by DNA sequencing.

Cell culture and DNA transfection

CHO-K1 cells were obtained from the Cell Resource Center for Biomedical Research, Institute of Development, Aging and Cancer, Tohoku University, and grown on a poly(D-lysine)-coated glass-bottomed culture dish (35 mm; MatTeK Corporation, Ashland, MA, USA) in phenol red-free DMEM (Gibco, Frederick, MD, USA) supplemented with 10% fetal bovine serum, 1% nonessential amino acid solution (Gibco), 2 mM L-glutamine (Sigma-Aldrich, St Louis, MO, USA), and 40 $\mu g \cdot mL^{-1}$ kanamycin. DNA (0.5 μg) consisting of equal amounts of each expression plasmid was introduced into CHO-K1 cells by the lipofection method, using FuGENE 6 transfection reagent (Roche, Basel, Switzerland). Cells were incubated for 40 h after transfection and observed with a FLIM microscope.

Immunofluorescence staining

HeLa cells were fixed with 3% formaldehyde and immunostained using rabbit polyclonal antibody against GAPDH (diluted 1 : 50) (Trevigen, Gaithersburg, MD, USA) or rabbit polyclonal antibody against PGK1 (diluted 1 : 50) (Abgent), followed by tetramethylrhodamine isothiocyanate (TRITC)-conjugated secondary antibody (diluted 1 : 100) (Santa Cruz Biotechnology, Santa Cruz, CA, USA).

Size exclusion chromatography and enzyme assays

Whole cell extracts of cells transfected with plasmids for GAPDH–citrine and PGK–cerulean were subjected to size exclusion chromatography using Superdex 200 and Superdex 75, respectively (GE Healthcare, Little Chalfont, UK). GAPDH and PGK activities were determined by the methods of Velick [22] and Yoshida [23], respectively.

Western blotting and immunoprecipitation

Whole cell extracts were prepared by mixing CHO-K1 cells transfected with plasmids encoding chimeric fluorescent proteins with 10 mM Hepes buffer (pH 7.9), containing 0.1 mM EDTA, 0.4 M NaCl, 1 mM dithiothreitol, 5% glycerol, and protease inhibitor cocktail (Nacarai Tesque, Kyoto, Japan). Proteins were resolved by 7.5–10% SDS/PAGE, and transferred to a nitrocellulose membrane (GE Healthcare). Rabbit polyclonal antibody against green fluorescent protein (GFP) (Takara Bio, Otsu, Japan) (diluted 1 : 1000), rabbit polyclonal antibody against GAPDH (diluted 1 : 1000) (Trevigen) and rabbit polyclonal antibody against PGK1 (diluted 1 : 500) (Abgent, San Diego, CA, USA) were used as the first antibodies. The antibody against GFP reacted with cerulean more strongly than with citrine. Horseradish peroxidase-linked goat anti-(rabbit IgG) (Vector Laboratories, Burlingame, CA, USA) was used as the second antibody. The membrane was developed with the ECL Plus detection system (GE Healthcare). CHO-K1 cells were transfected with plasmids for HA-tagged GAPDH and FLAG-tagged PGK, harvested, lysed, and exposed to FLAG–affinity agarose beads (Sigma-Aldrich) that had been pretreated with antibody against FLAG. Proteins bound to washed beads were eluted, boiled, and separated by SDS/PAGE. After electrophoresis, the proteins were blotted onto a nitrocellulose membrane and probed with antibody against HA.

FLIM measurements

FLIM measurements were performed as described previously [24]. The emission lifetimes of fluorescent cells were measured on an inverted microscope (Zeiss: Axiovert 135, ×100 oil immersion objective with numerical aperture of 1.3) equipped with a disk anode microchannel plate photomultiplier (Europhoton, Berlin, Germany), which can detect photons in a time-resolved and space-resolved fashion by using a time-correlated single-photon-counting technique. Spatial resolution can be obtained with a quadrant anode, the details of which are given elsewhere [25,26]. The excitation source was a 410 nm picosecond diode laser (full width at half-maximum of 78 ps; LDH-P-C-400, PicoQuant, Berlin, Germany), which illuminates a relatively large area of approximately 100 μm in diameter, and was operated at a repetition rate of 10 MHz. Average excitation power was estimated to be $\sim 15\ \mathrm{mW \cdot cm^{-2}}$, which is equivalent to the single-photon-counting level. The instrumental response function (IRF) was recorded as reflected excitation light, as shown in Figs 2 and 3. Fluorescence from live cell samples incubated at 37 °C was sequentially collected at 475 ± 25 nm for cerulean and 575 ± 25 nm for citrine by bandpass filters at a count rate below about 0.5 counts $(\mathrm{pixel \cdot s})^{-1}$. The acquisition time of the donor and acceptor fluorescence was about 20 min, giving rise to peak values of approximately 2000 photon counts. Fluorescence lifetime data were analyzed using global analysis with multiexponential decays [27].

Statistical analysis

The statistical significance was determined using Student's *t*-test, and *P*-values < 0.05 were considered to be significant.

Acknowledgements

We thank K. Mizumoto (Kitasato University) for the generous gift of human PGK1 cDNA. This work was supported in part by a Grant-in-Aid for research from the Ministry of Education, Culture, Sports, Science and Technology of Japan. K. Kemnitz acknowledges support from NMP4-2005-013880.

References

1 Srivastava DK & Bernhard SA (1986) Metabolite transfer via enzyme–enzyme complexes. *Science* **234**, 1081–1086.
2 Srere PA (1987) Complexes of sequential metabolic enzymes. *Annu Rev Biochem* **56**, 89–124.
3 Eikmanns BJ (1992) Identification, sequence analysis, and expression of a Corynebacterium glutamicum gene cluster encoding the three glycolytic enzymes glyceraldehyde-3-phosphate dehydrogenase, 3-phosphoglycerate kinase, and triosephosphate isomerase. *J Bacteriol* **174**, 6076–6086.
4 Shih S-C & Claffey KP (1998) Hypoxia-mediated regulation of gene expression in mammalian cells. *Int J Exp Pathol* **79**, 347–357.
5 Malhotra OP, Prabhakar P, Sen Gupta T & Kayastha AM (1995) Phosphoglycerate-kinase–glyceraldehyde-3-phosphate-dehydrogenase interaction. Molecular mass studies. *Eur J Biochem* **227**, 556–562.
6 Fokina KV, Dainyak MB, Nagradova NK & Muronetz VI (1997) A study on the complexes between human erythrocyte enzymes participating in the conversions of 1,3-diphosphoglycerate. *Arch Biochem Biophys* **345**, 185–192.
7 Ashmarina LI, Muronetz VI & Nagradova NK (1985) Yeast glyceraldehyde-3-phosphate dehydrogenase. Evidence that subunit cooperativity in catalysis can be controlled by the formation of a complex with phosphoglycerate kinase. *Eur J Biochem* **149**, 67–72.
8 Sukhodolets MV, Muronetz VI & Nagradova NK (1987) Interaction between D-glyceraldehyde-3-phosphate dehydrogenase and 3-phosphoglycerate kinase labeled by fluorescein-5′-isothiocyanate: evidence that the dye participates in the interaction. *Biochem Biophys Res Commun* **161**, 187–195.

9 Weber JP & Bernhard SA (1982) Transfer of 1,3-diphosphoglycerate between glyceraldehyde-3-phosphate dehydrogenase and 3-phosphoglycerate kinase via an enzyme–substrate–enzyme complex. *Biochemistry* **21**, 4189–4194.
10 Vas M & Batke J (1981) Evidence for absence of an interaction between purified 3-phosphoglycerate kinase and glyceraldehyde-3-phosphate dehydrogenase. *Biochim Biophys Acta* **13**, 193–198.
11 Vas M & Batke J (1990) Kinetic misinterpretation of a coupled enzyme reaction can lead to the assumption of an enzyme–enzyme interaction. The example of 3-phospho-D-glycerate kinase and glyceraldehyde-3-phosphate dehydrogenase couple. *Eur J Biochem* **191**, 679–683.
12 Ikemoto A, Bole DG & Ueda T (2003) Glycolysis and glutamate accumulation into synaptic vesicles. Role of glyceraldehyde phosphate dehydrogenase and 3-phosphoglycerate kinase. *J Biol Chem* **278**, 5929–5940.
13 Singh P, Salih M, Leddy JJ & Tuana BS (2004) The muscle-specific calmodulin-dependent protein kinase assembles with the glycolytic enzyme complex at the sarcoplasmic reticulum and modulates the activity of glyceraldehyde-3-phosphate dehydrogenase in a Ca2+/calmodulin-dependent manner. *J Biol Chem* **279**, 35176–35184.
14 Wallrabe H & Periasamy A (2005) Imaging protein molecules using FRET and FLIM microscopy. *Curr Opin Biotechnol* **16**, 19–27.
15 Becker W, Bergmann A, Hink MA, Konig K, Benndorf K & Biskup C (2004) Fluorescence lifetime imaging by time-correlated single-photon counting. *Microsc Res Tech* **63**, 58–66.
16 Rizzo MA, Springer GH, Granada B & Piston DW (2004) An improved cyan fluorescent protein variant useful for FRET. *Nat Biotech* **22**, 445–449.
17 Heikal AA, Hess ST, Baird GS, Tsien RY & Webb WW (2000) Molecular spectroscopy and dynamics of intrinsically fluorescent proteins: coral red (dsRed) and yellow (Citrine). *Proc Natl Acad Sci USA* **97**, 11996–12001.
18 Tramier M, Zahid M, Mevel J-C, Masse M-J & Coppey-Moisan M (2006) Sensitivity of CFP/YFP and GFP/mCherry pairs to donor photobleaching on FRET determination by fluorescence lifetime imaging microscopy in living cells. *Microsc Res Tech* **69**, 933–939.
19 Jindal HK & Vishwanatha JK (1990) Functional identity of a primer recognition protein as phosphoglycerate kinase. *J Biol Chem* **265**, 6540–6543.
20 Siegler KM, Mauro DJ, Seal G, Wurzer J, deRiel JK & Sirover MA (1991) Isolation and characterization of the human uracil DNA glycosylase gene. *Proc Natl Acad Sci USA* **88**, 8460–8464.
21 Berry MD & Boulton AA (2000) Glyceraldehyde-3-phosphate dehydrogenase and apoptosis. *J Neurosci Res* **60**, 150–154.
22 Velick SF (1955) Glyceraldehyde-3-phosphate dehydrogenase from muscle. *Methods Enzymol* **1**, 401–406.
23 Yoshida A (1975) Human phosphoglycerate kinase. *Methods Enzymol* **42**, 541–547.
24 Kinoshita K, Goryo K, Takada M, Tomokuni Y, Aso T, Okuda H, Shuin T, Fukumura H & Sogawa K (2007) Ternary complex formation of pVHL, elongin B and elongin C visualized in living cells by a FRET–FLIM technique. *FEBS J* **274**, 5567–5575.
25 Kemnitz K, Pfeifer L, Paul R & Coppey-Moisan M (1997) Novel detectors for fluorescence lifetime imaging on the picoscecond time scale. *J Fluoresc* **7**, 93–98.
26 Kemnitz K, Pfeifer L & Ainbund MR (1997) Detector for multichannel spectroscopy and fluorescence lifetime imaging on the picosecond timescale. *Nucl Instrum Methods Phys Res A* **387**, 86–87.
27 Beechem JM (1989) A second generation global analysis program for the recovery of complex inhomogeneous fluorescence decay kinetics. *Chem Phys Lipids* **50**, 237–251.

Supporting information

The following supplementary material is available:
Fig. S1. Subcellular localization and enzymatic activities of citrine–GAPDH and cerulean–PGK.
Fig. S2. Error analysis of two-exponential fitting for decay curves.

This supplementary material can be found in the online version of this article.

Please note: As a service to our authors and readers, this journal provides supporting information supplied by the authors. Such materials are peer-reviewed and may be re-organized for online delivery, but are not copy-edited or typeset. Technical support issues arising from supporting information (other than missing files) should be addressed to the authors.